



Numerical modeling of umbrella arch technique to reduce tunnelling induced ground movements

Hamid Zarei¹ · Parviz Moarefvand¹ · Ebrahim F. Salmi²

Received: 19 August 2018 / Accepted: 27 April 2019 / Published online: 8 May 2019
© Springer-Verlag GmbH Germany, part of Springer Nature 2019

Abstract

One of the most important aspects of tunnelling in soft grounds is to reduce any possible adverse environmental impact. That is, pre-supporting techniques are found to boost tunnelling advance speed whilst, at the same time, keeping the environmental consequences due to tunnelling process appreciably low. The umbrella arch method is one of the most common ground pre-supporting techniques used in tunnelling. The interactions between the ground and umbrella arches are very complex. There are also several parameters affecting the performance of the umbrella arch technique. Sophisticated numerical modeling is, therefore, required to gain a proper understanding of the mechanism of ground movement based on the umbrella arch method. In this paper, the role of the pipe roofing and face bolting on the stabilization of the northern portal of Sabzkooh tunnel is assessed using three-dimensional (3D) numerical method. Furthermore, the effects of design parameters such as the pipes installation angle, the pipes diameter and the transverse spacing of pipes on the performance of umbrella arch system are investigated through numerical modeling. The vertical displacements of the tunnel crown and the internal forces induced in the initial support system are extracted from the numerical modeling and are carefully assessed to identify the role of the pre-supporting methods. The outcomes of the numerical modeling demonstrate that when pipe roofing and face bolts are utilized, the tunnel convergence decreases and the induced axial forces in the initial support system tend to increase. These clearly highlight the role of pre-supporting technique on stabilizing the tunnel and transferring ground loads to the support measure. Results also show that reduction in the installation angle and transverse spacing of pipes and increasing the diameter of pipes can all considerably reduce the tunnel crown displacement while they increase the maximum induced axial forces in the initial support system. Stability analysis using bearing capacity diagrams also indicates that the initial support system with different configurations of pipe roofing and face bolts at different cross sections along the tunnel alignment is fairly sturdy and robust against the applied loads.

Keywords Tunnelling · Weak ground · Pre-supporting · Umbrella arch method · Numerical modeling

Introduction

One of the most important concerns during tunnelling in soft grounds is maintaining the stability of the structure. Low bearing capacity and dealing with large excavation induced deformations are among the main challenges are exposed during tunnelling in weak grounds (Chakeri and Unver

2014). There are, variety of methods available to keep the tunnel face stable in soft grounds such as breaking down the tunnel face area into small manageable pieces, using shorter advance length, implementing ground improvement and pre-supporting techniques. In particular, using pre-supporting methods reduces the adverse environmental impacts of tunnelling (e.g., ground surface settlement and the size of the zone affected by the excavation). Umbrella arch method is, indeed, one of the most applicable pre-supporting methods.

To ensure the stability of tunnels in weak grounds, it is highly required to control and manage the excavation induced ground movements. Uncontrolled deformations can jeopardize the tunnel stability (Ocak 2013, 2014). Tunnelling induces ground movements, which occur before the installation of the initial support system. In other words,

✉ Hamid Zarei
hamid.zarei@aut.ac.ir

¹ Faculty of Mining and Metallurgical Engineering, Amirkabir University of Technology, Tehran, Iran

² Independent Researcher and Former Postgraduate Student, Faculty of Mining and Metallurgical Engineering, Amirkabir University of Technology, Tehran, Iran

a considerable proportion of the excavation induced deformations released during tunnelling. Umbrella arch methods and face bolting technique are used to minimize the pre-convergence of the tunnel walls and the inward movements of the tunnel face. These not only result in appreciably smaller deformations around the tunnel, but also considerably increase the tunnel stability (Aksoy and Onargan 2010; Salmi et al. 2017). Where excavation is performed in urban areas, the ground movements imposed by tunnelling activities can affect the stability of surface structures and infrastructure. A precise estimation of induced settlements is needed to design a proper mitigation system to control and reduce the undesirable effects of tunnelling to acceptable levels (Ercelebi et al. 2011; Ocak 2014).

Pipe roofing is one of the umbrella arch methods where steel and/or fiberglass pipes are installed around the tunnel periphery with an angle around 5° – 10° from the horizon. In the majority of reported cases of pipe roofing, the diameter and wall thickness of the pipes vary from 60 to 200 mm and 4 to 8 mm, respectively (Volkman et al. 2006). The pipes are usually 12–15 m in length where some degree of overlap is considered on the next round of pipes to maintain the face stability (Peila and Pelizza 2005; Volkman et al. 2006). A schematic view of the pipe roofing method is illustrated in Fig. 1. The pipes are installed and the annulus spaces between them and the surrounding ground are grouted. Then tunnelling is performed beneath the provided arch roof. It is notable that the main aim of grouting inside the pipes and in the annulus space between the pipes and the surrounding ground is to increase the bending strength of the pipes and to increase load transmission capability between the ground and the support system (Volkman and Schubert 2008). The area around the pipes is, therefore, strengthened because of the grout penetrating or filling the fractures due to which the

umbrella system can be effective even in transversal direction (Muraki 1997).

Several reports on the successful application of the umbrella arch methods under harsh ground conditions have been published worldwide (Aydin et al. 2004; Ocak 2008; Elyasi et al. 2016). However, the real mechanisms of ground movement, achieved by the umbrella arch technique, have not been well clarified, yet. There has, therefore, been a long standing interest to identify the pre-supporting mechanisms of the umbrella arch method. The previous studies may be divided into three main groups, include but are not limited to, analytical studies (Wang and Jia 2008, 2009; Zhang et al. 2010), experimental tests (e.g., centrifuge tests) (Shin et al. 2008; Juneja et al. 2010) and numerical modeling (Volkman et al. 2006; Song et al. 2013; Schumacher and Kim 2013; Zhang et al. 2014; Oke et al. 2014; Salmi et al. 2015, 2017).

A few researchers developed analytical techniques to assess the effects of umbrella arches on the stability of tunnels (Bruce et al. 1987; Peila and Pelizza 2005; Pizzarotti 2001). Although analytical approaches provide a simple understanding of the mechanisms, of pre-supporting through pipe roofing technique, they normally overlook the real complex interaction between individual pipes and their surrounding ground. In the majority of the cases, pipes are simplified to cantilever or supported beams. Therefore, these approaches fail to provide an accurate estimation of the behavior of pipe roofing system during tunnelling. It is also noted that due to the existence of several interrelated factors, finding closed form solutions for explaining the behavior of the umbrella arch technique is limited to simplified cases. Such approaches have not, therefore, resulted in noticeable achievements. In particular, because umbrella arch system is installed prior to the excavation and ahead of the tunnel face, analytical approaches are not capable of capturing the real behavior of such supports. Although experimental tests (e.g., centrifuge tests) have provided tunnel engineers with a good insight of the behavior of umbrella arch, their application in the design of real life project is limited to a certain level, mainly due to scale effects.

The literature review of previous numerical studies, in this field, also reveals that the effect of umbrella arch approach mainly included by defining an equivalent area around the tunnel roof which is strengthened by the installation of pipes, and the injection of grout through the pipes and around them (Hefny et al. 2004; Hoek 2004; Salmi et al. 2017). In other words, the properties of the soil/rock mass in the affected zone are improved based on the relative area of the grout and the steel pipes. This approach has well been explained by Hoek (2004). Additionally, in a few of the previous studies, the pipes in the umbrella arch, the surrounding ground, and the support measures (e.g. shotcrete) have all numerically been simulated by defining different

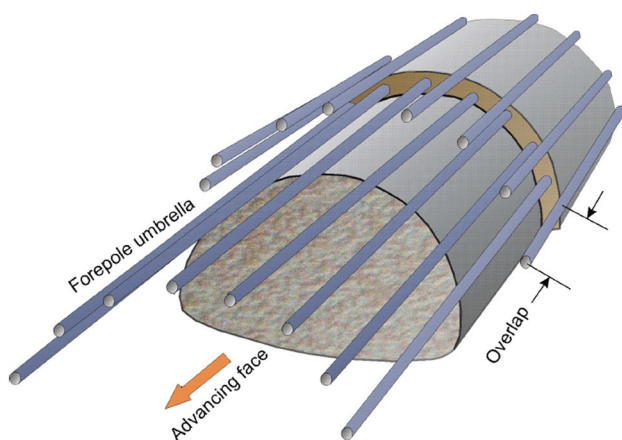


Fig. 1 A schematic view of tunnel excavation under the protective umbrella arch. (Courtesy of Hoek 2004)

specific zones with mechanical properties equivalent to the counterparts in the site (Ahuja and Sterling 2008; Barla and Bzowka 2013; Coulter and Martin 2006; Coulter 2004). The main problem with this approach is that extracting the moments, and the shear and internal forces developed in the pipes could be very challenging. In other words, in most of the existing literature on the numerical modeling of umbrella arch technique, an equivalent approximation of the composite medium, consisting of pipes, grout and surrounding ground, was considered in the analyses. It is worth noting that such approximation of the geotechnical properties of the composite medium may involve a considerable level of uncertainties and ambiguities.

In this paper, the effects of the design parameters of pipe roofing system (e.g., pipes installation angle, pipes diameter, pipes transverse spacing and pipes overlapping length), on the performance of pre-supporting system are assessed through three-dimensional (3D) numerical modeling. It is noted that in this research pipes are individually modeled independently of the surrounding ground. The northern portal of Sabzkooh water conveyance tunnel is studied as a case history. Tunnelling in this area resulted in several environmental issues. In particular, collapse of the tunnel face generated several sinkholes in the area (Eftekhari et al. 2014; Taromi et al. 2017). The excavation of Sabzkooh tunnel also affected the discharge of surface springs in the area. Similar environmental issues because of tunnelling have been well reported in relevant references (Salmi et al. 2015, 2017; Türkmen and Özgüzel 2003). Both the tunnel crown

vertical displacements and the magnitude of internal forces induced in the initial support system are recorded during the numerical modeling. These data are then used to evaluate the role of the pre-supporting system. For the sake of result validation of the numerical model, the analytical method proposed by Schwartz and Einstein (1980) for computing the internal forces in the initial support system is also used and compared against the outcomes of the numerical modelings.

Case study of Sabzkooh tunnel

Sabzkooh tunnel has 10,600 m in length and 4.52 m in excavated diameter, is to be constructed in Chaharmahal and Bakhtiari Province, Iran. The northern portal of the tunnel is approximately located at 400 m to the southern bank of Choghakhor Lake. The tunnel is meant to act as a duct to convey water from Sabzkooh Dam (southern portal) to Choghakhor Lake (northern portal). Three boreholes were drilled at the northern portal to obtain the geotechnical parameters needed for the design of support system and planning the excavation method. Typical sections of the borehole logs and the outcomes of soil characterization are shown in Fig. 2. The log data obtained from the boreholes indicated that the surrounding ground at the northern portal consists of alluvium, mostly clay (CL), clayey sand (SC) and silt (ML) and is consistent in the first 200 m of the tunnel length. Due to the low strength of the surrounding ground, it was planned to excavate this section of the tunnel using

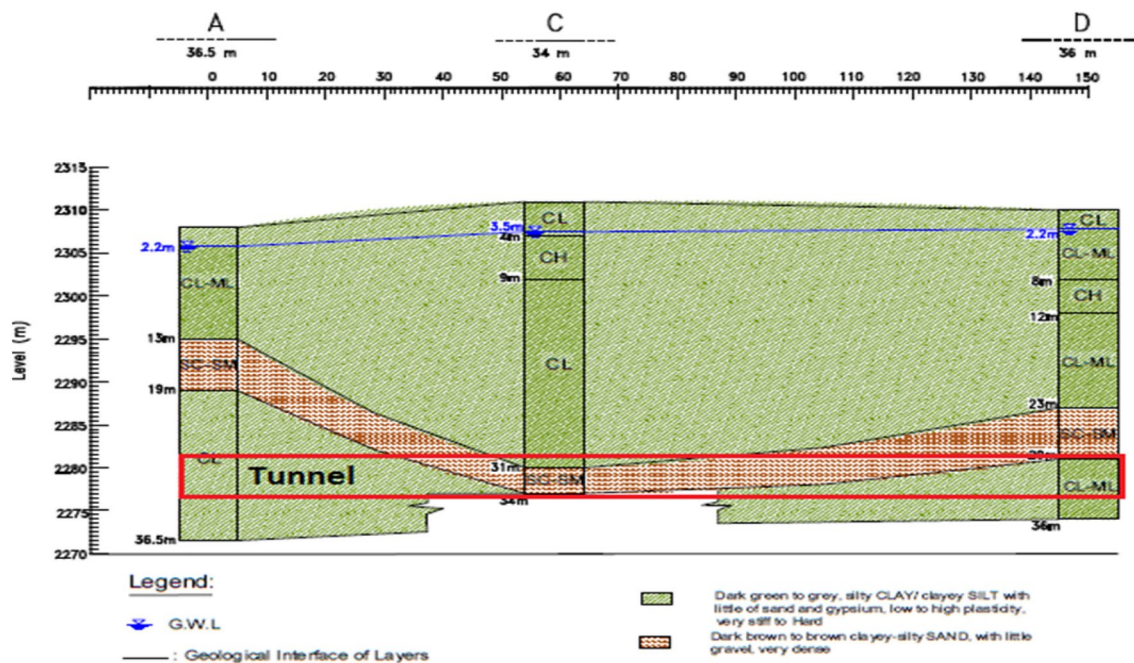


Fig. 2 Borehole logs and soil characterization in the northern portal of the Sabzkooh tunnel (Taromi et al. 2017)

traditional excavation methods preparing the portal for the tunnel boring machine (TBM) to launch and excavate the rest of the tunnel in strong sedimentary rocks (Eftekhari et al. 2014; Taromi et al. 2015).

The high Zagros, a special structural part of the Zagros zone which is known for its transverse strike-slip and thrust faults, hosts the tunnel. In the study area, sedimentary bedding at the beginning of the tunnel has been widely disturbed by the interaction of Solaghan thrust fault featuring a 40°–65° dip angle (Taromi et al. 2017). The longitudinal geological profile of the tunnel route is given in Fig. 3.

The geological and geotechnical characteristics of the tunnel area have very well been investigated and reported in the relevant references (Eftekhari et al. 2014; Aliabadian et al. 2015; Taromi et al. 2017). The above-mentioned references were used, in this study, to extract the geotechnical

data required for performing numerical modeling. Table 1 shows the geotechnical parameters of different soil layers. Additionally, the geometry of the numerical model along with the stratigraphy of the area incorporated in the model is presented in Fig. 4. As can be seen in this figure, only

Table 1 Geotechnical characteristics of different layers

Layer number	1	2	3
Depth of the layers (m)	0–12	12–17	17–45
Soil type	CL–ML	SC–MC	CL
Internal friction angle (°)	22	26	22
Cohesion (kPa)	13	5	24
Dry density (kN/m ³)	18	19	18
Elasticity modulus (MPa)	40	50	40

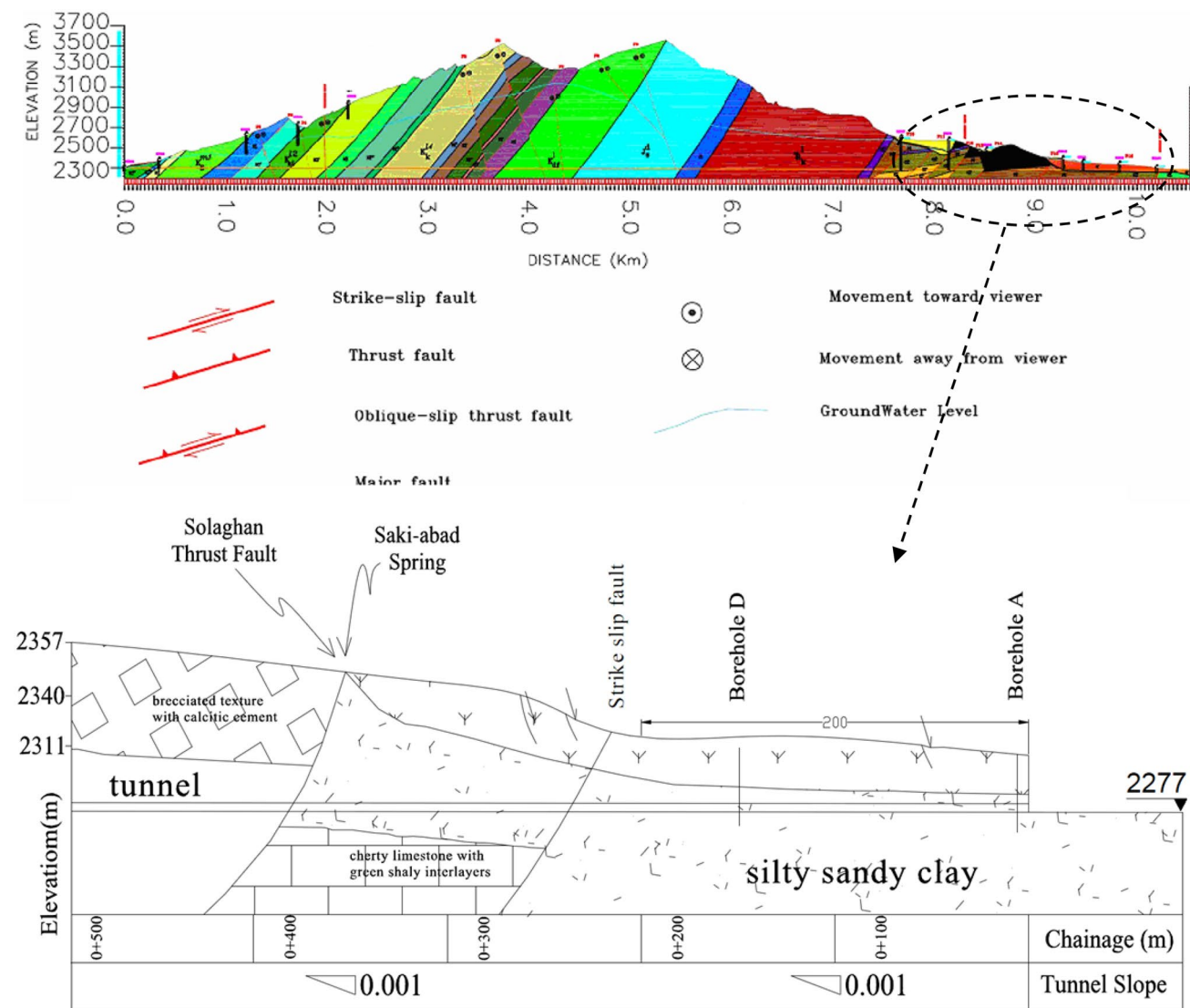


Fig. 3 The geological profile of the Sabzkooh tunnel (RWC C&BP 2009)

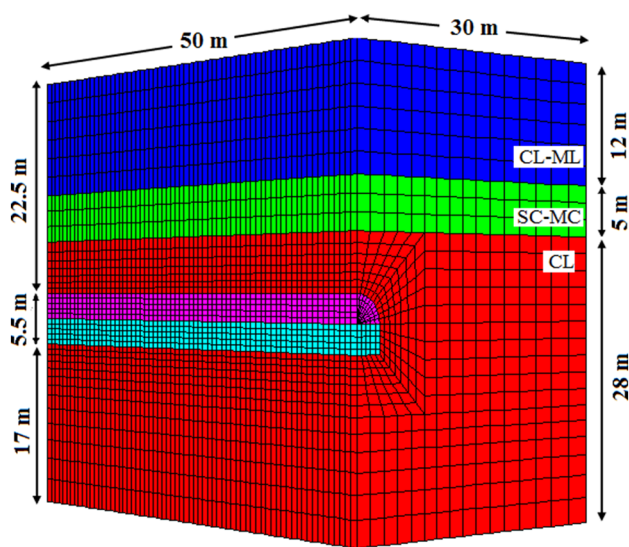


Fig. 4 The model geometry as well as the bedding condition

the right half of the tunnel is modeled due to the symmetry condition. This can considerably reduce the computational efforts.

It is notable that a chimney collapse in the tunnel crown happened in chainage + 33.8 m from the northern portal, expanding vertically to the ground surface with maximum 18.7 m in height and resulting in a large sinkhole on the surface (Eftekhari et al. 2014). Figure 5 depicts two views of the first tunnel collapse and the sinkhole formation incident occurred close to the tunnel portal. Figure 6 also shows the locations of all instabilities resulted in developing sinkholes

during conventional excavation of the first lot of the Sabzkouh tunnel.

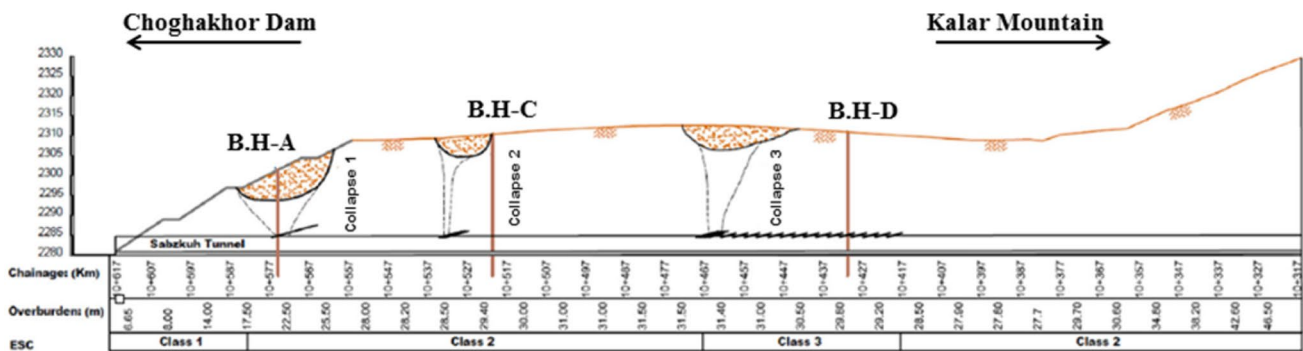
With that collapse occurred, the chimney created had to be filled up with proper material and some treatment measure was to be taken to prevent further failure and to continue the excavation process. Pipe roofing and face bolting systems were chosen as proper pre-supporting technique of the tunnel due to their high flexibility and practical applicability.

Numerical modeling

The northern portal of Sabzkouh tunnel has a horseshoe shape cross section with 5.5 m span, 5.5 m height, and 22.5 m overburden on top. These dimensions are used to build up the numerical model (see Fig. 4). Numerical models are constructed based on the principal rules proposed by Starfield and Cundall (1988). According to this approach, oversimplification of the problem or including excessive elaboration and details in numerical model both should be avoided. The well-known Finite Difference package, FLAC^{3D}, was selected for performing numerical modeling (Itasca Consulting Group 1997). Constant tetrahedral and hexahedral formed strain-rate type elements (CSTE) are used to numerically model the tunnel structure. The tetrahedral elements are used to simulate the tunnel core which is then excavated during the numerical modeling. The finer hexahedral elements are, however, used to simulate the surrounding ground, adjacent to the tunnel which is the region of interest. These finer hexahedral meshes are, indeed, used to make sure that the plastic behavior of the surrounding



Fig. 5 The first tunnel collapse occurred in the northern portal of Sabzkouh tunnel (Eftekhari et al. 2014)



The first collapse



The second collapse



The third collapse

Fig. 6 A view of all instabilities resulted in developing sinkholes in the Sabzkuh tunnel (Taromi et al. 2017)

rock is accurately replicated. The model finally includes 25,281 elements and 27,918 nodal points. The elastic perfectly plastic Mohr–Coulomb failure criterion is also used to simulate the non-linear behavior of the soil. The lateral stress ratio is calculated using the well-known Jaky (1948)’s equation based on the internal friction angle of the soil mass ($K = 1 - \sin \varphi$).

There exist two main strategies for numerical modeling of the umbrella arch system and investigating the role of the pre-supporting systems on stabilizing the tunnel. The first strategy is based on using an equivalent approximation of the composite medium consisting of pipe-roof, grout and the

reinforced surrounding ground. To do so, the geotechnical characteristics of the ground in this area are improved (Hoek 2004; Salmi et al. 2015, 2017). The second approach is to model the pipes individually. Hefny et al. (2004) studied the influence of different methods of umbrella arch approximation using FDM on the shape and magnitude of ground movements during tunnelling. They showed that employing different methods of approximation may significantly influence the values and the shape of ground settlement as well as the vertical displacement of the tunnel crown. According to Volkmann et al. (2006), pipes may carry the load to the side of the tunnel longitudinally while transverse load

bearing may manifest itself through pre-supporting system such as grouted columns. Therefore, pipes should carefully be modeled by means of 3D numerical modeling.

In this study, the pipes in the umbrella arch are modeled using structure elements, known as pile, which are embedded in the non-linear surrounding soils. The main purpose of utilizing such elements is to precisely simulate the interactions between the soil mass and the pipes in the umbrella arch. Pile elements are capable of replicating the induced internal forces in the pipes (such as axial force and bending moment), the frictional interaction developed between the pipes and the surrounding ground, as well as the shear and normal stress distribution along the pipes. Both occurred normal and shear-directed frictional interaction with the surrounding media can be simulated using pile structure elements.

Connectivity between the source node and the other surrounding node or zones can simply be considered in numerical modeling. When a pile structure element is used, links between pile nodes and the volume element grid-points are automatically created. There are two separate nodes at the connection of pipes (simulated using pile structure element) and the initial support system (simulated using shell structure element). A node-to-node link was considered in this study to reflect the connection between pipes and the support measure. In practice, to install the umbrella arch system, in the Sabzkooch tunnel, the beginning of the pipes are mounted on the initial support system (steel frames) in designed layout and the pipes are welded to the steel frame at the intersection points with steel arches to stay in their locations. Therefore, a node-to-node link created at the junction of the pipes and the initial support system is fixed in all direction to represent this condition. The connection condition is, therefore, considered to properly analyze the load transmission between pipes and the initial support system.

In practice, pipes are hollow at the initial stage of installation. Later, inside the pipes and the annulus space between the pipes and the surrounding ground are grouted. The determination of the geometrical characteristics (e.g., the area and moment of inertia) of the equivalent cross section of pipes filled up with grout are performed based on the elasticity module of both grout and steel pipes, and using numerical modeling. To do so, the steel pipe is considered as the based material and the grout is transformed to an equivalent amount of steel according to the ratio of their elasticity module. Further details related to this widely used approach, which is known as *computing the transformed section of combined materials*, can be found in relevant references (Popov 1990). Additionally, the grout injected in the annulus space between the pipes and the surrounding ground is represented numerically as a spring-slider system located between the pipes and the surrounding soil. The grout has 24° friction angle and the grout cohesive strength per unit

Table 2 Mechanical properties of pipe roof elements

Parameter	E_p	ν_p	A_p^*	I_p^*
Unit	GPa	–	m^2	m^4
Value	210	0.30	1.94×10^{-3}	2.18×10^{-6}

*These parameters vary based on the size of pipes and the injected grout

Table 3 Mechanical properties of face bolt elements (Wong et al. 1999)

Parameter	E_{fb}	A_{fb}	σ_{yfb}
Unit	GPa	m^2	MPa
Value	40	8.05×10^{-4}	500

length and the grout stiffness per unit length are 50 (kN/m) and 5×10^2 (MPa), respectively.

The fiberglass face bolts are also simulated using a specific type of structure element which can provide a shearing resistance based on the mechanical properties of grout materials along the face bolt's length. The mechanical properties of the pipe roof elements and the face bolts are shown in Tables 2 and 3:

where in Table 2, E_p , ν_p , A_p , and I_p , are the elastic modulus, the Poisson's ratio, the cross section area and the second moment of pipes used in the umbrella arch, respectively.

In Table 3, E_{fb} , A_{fb} and σ_{yfb} denote the elasticity modulus, the cross section area and the tensile yield strength of the face bolts, respectively.

Excavation in the area indicated that the unsupported tunnel span is around 0.75 m. Therefore, the tunnel advance round is assumed to be 0.75 m which is also the same as the lateral spacing between the steel frames. In the numerical modeling, the tunnel excavation is advanced up to 24 m length. Excavation is modeled in a full-face fashion and the initial support system of the current excavated area is installed with the onset of the upcoming excavation step. The temporary composite support system consists of 200 mm shotcrete which has been reinforced with two layers of wire mesh ($\Phi 100$ mm @ 5 mm), and steel frames with 0.75 m lateral spacing. The approach proposed by Hoek et al. (2008) and later by Carranza-Torres and Diederichs (2009) is used to numerically simulate this composite support system. The aforementioned approach is used to estimate the parameters of the homogenized equivalent section representing the entire composite support measures. Then the loads and stresses on the equivalent support system are extracted from the numerical modeling.

Pipes are also modeled with different diameters (shown here as ' d '), length of 12 m, overlapping length of 3.75 m, three different transverse spacing (shown here as ' s ') of

30 cm, 40 cm, 50 cm, and installation angles (shown here as ‘angle’) of 5°, 10° and 12° with respect to horizon. Fiberglass face bolts have 32 mm in diameter, 15 m in length and overlapping length of 6 m and are installed in three rows with 1.0 m × 1.0 m square grid. That is, the model contains three stages of pipe roofing installed, and three stages of face bolts. The tunnel profile along with the initial support system, the pipe roofing system and face bolts are illustrated in Fig. 7. Since the northern portal of Sabzkooh tunnel is located in soil, the tunnel and the surrounding ground are modeled as a continuous medium using Finite Difference Method (FDM). Overall, 12 numerical models have been constructed to investigate the effects of design parameters of the performance of the pipe roofing system.

Overall influence of the pipe roofing system and face bolts

To investigate the role of pre-supporting methods, two scenarios are considered. In the first scenario, the pre-supporting system is installed while the second case does not include pre-supporting system. The longitudinal profile of the tunnel crown vertical displacements and the longitudinal profile of the ground surface settlement for the above-mentioned scenarios are shown in Figs. 8 and 9, respectively. Illustration of these figures shows that with pipe roofing and face bolts installed, the vertical displacements of the tunnel crown and the ground surface settlement significantly drop. The vertical displacements of the tunnel crown show more than 50% decrease at some locations along the tunnel alignment. As can be seen in Fig. 8, there are two relative minimum on the curve at 9 m and 17 m where displacements are clearly lowered representing a new set of the pipe roofing system installed and the effect of the overlapping of a new and old set of pipes and bolts.

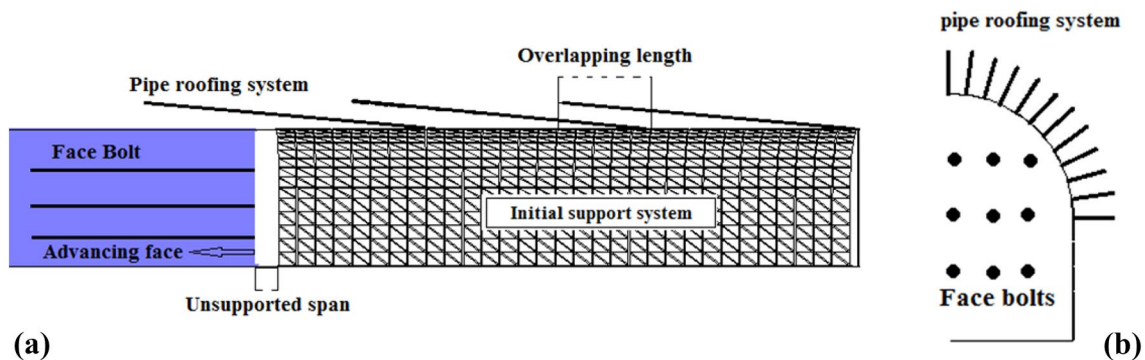


Fig. 7 Longitudinal (a) and cross section (b) of the tunnel along with the initial support system, pipe roofing and face bolts

Fig. 8 Vertical displacements of the tunnel crown in different scenarios #1 with pre-supporting #2 without pre-supporting

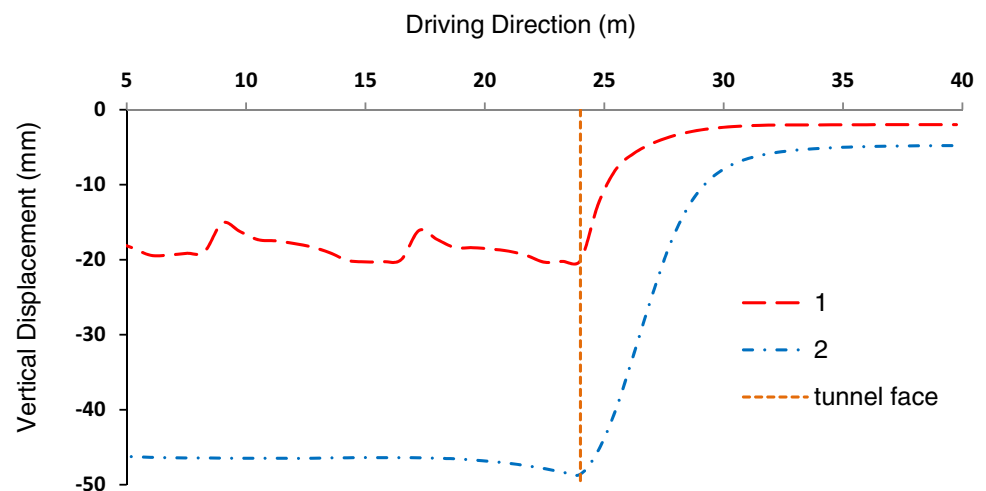
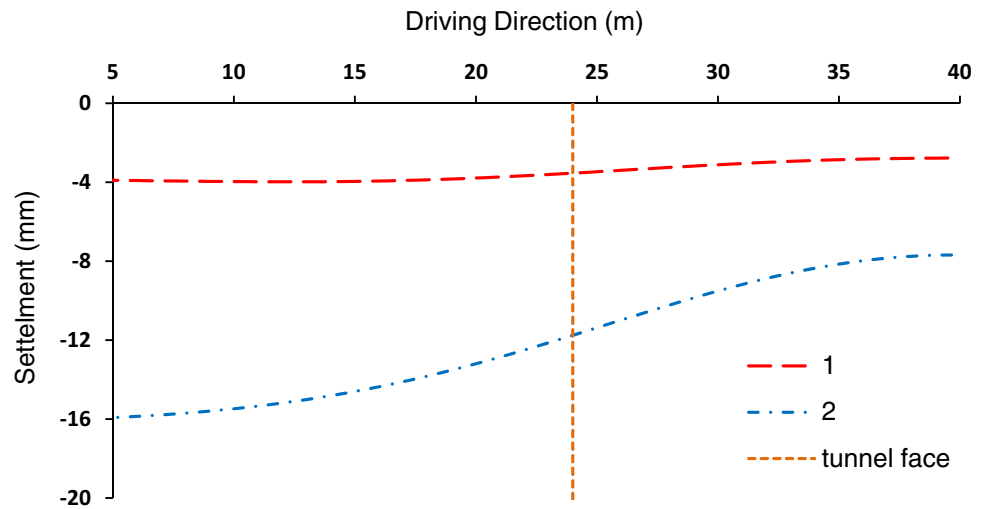


Fig. 9 Ground surface settlement for different scenarios #1 with pre-supporting, and #2 without pre-supporting



The induced axial force in the initial support system with cross section located at 10 m is compared for the two scenarios shown in Fig. 10. When the pre-supporting system is installed, the induced axial forces in the initial support system shows approximately 50% increase which is consistent with the fact that lower rate of displacements is observed with the presence of pre-supporting system because of transferring loads to the initial support system. The contours of vertical displacements in the vicinity of the tunnel for the aforementioned cases are shown in Fig. 11.

Investigating the role of parameters involved in pipe roofing system design

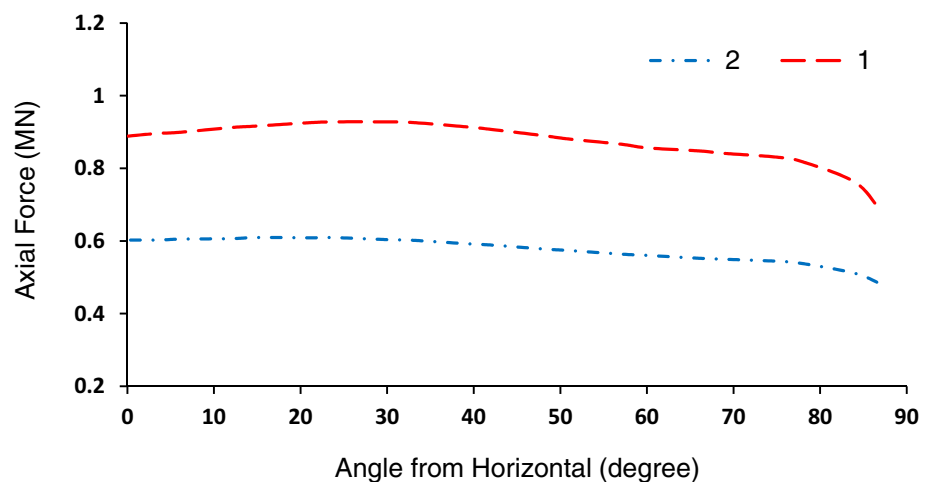
Design parameters are mainly controlled by each project constraints. This section is dedicated to investigating the role of a few design parameters on the performance of the pipe roofing system. The main parameters considered in this section are the installation angle, the transverse spacing

between pipes, and the diameter and overlapping length of pipes. The vertical displacements of the tunnel crown as well as the maximum induced internal forces in the initial support system are recorded to examine the role of the above-mentioned design parameters on the system performance. Regardless of how the design parameters are varied in the models, face bolts maintain with 15 m of length and 6 m of overlapping length, with the configuration shown earlier in Fig. 7.

Assessing the role of the installation angle of the pipes

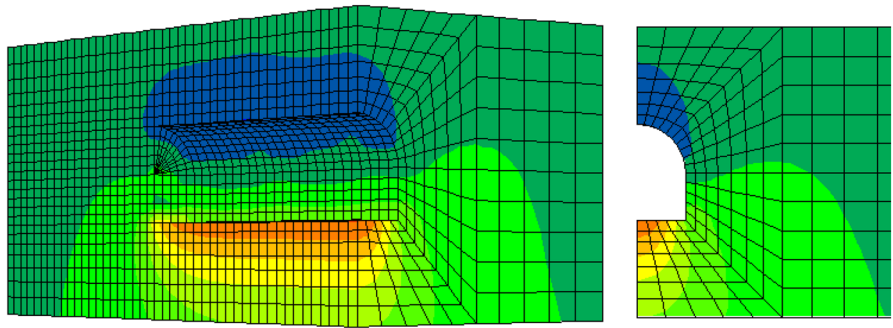
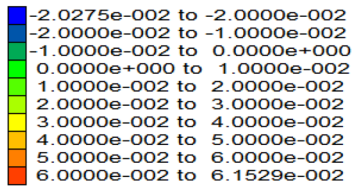
To investigate the effect of installation angle variation, three different installation angle of 5°, 10° and 12° are implemented in the numerical modeling while the constant diameter of 101 mm and constant transverse spacing of 40 cm are considered for the pipes. Outcomes of the analysis show that the larger the installation angle, the more the vertical displacements of the tunnel crown. The diagrams of the vertical

Fig. 10 Axial forces induced in the initial support system in different scenarios #1 with pre-supporting, and #2 without pre-supporting



1: with pre-supporting

Contour of vertical displacement
unit: m



2: without pre-supporting

Contour of vertical displacement
unit: m

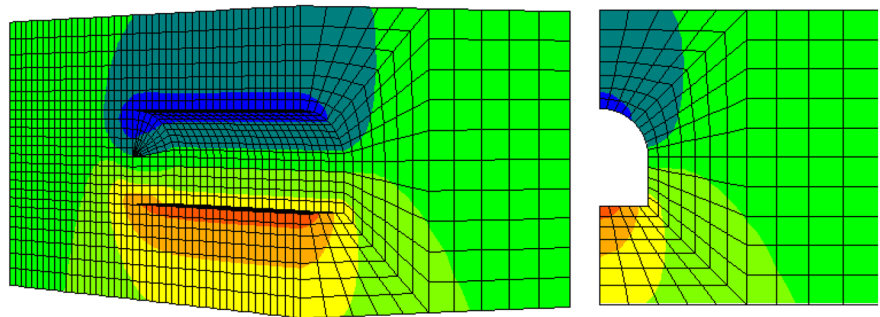
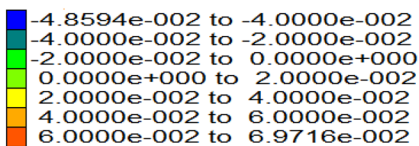


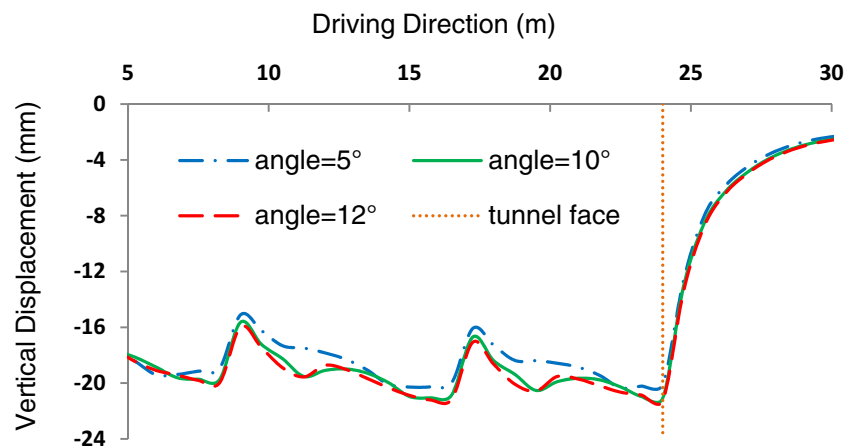
Fig. 11 Contours of vertical displacement around the tunnel in different modeling scenarios (perspective and cross section view in chainage 14 m)

displacements of the tunnel crown for different installation angles are presented in Fig. 12. Outcomes show that the increase in the installation angle from 5° to 12° with the extension of 11 m in longitudinal direction may lead to an increase of 12% in the vertical displacements. Results of the analyses also show that the difference between vertical displacements are not similar along the entire length of the profiles (the maximum vertical displacement difference occurred in 11 m and 19 m in the longitudinal direction).

To evaluate the effect of the installation angle variation on the induced maximum internal forces in the initial support

system, maximum internal forces associated with different installation angles are calculated in different cross sections. These sections include: the starting section of pipes of the second stage (a 10-m section namely A–A), the middle section of pipes of the second stage (a 14-m section namely B–B) and the ending section of pipes of the second stage (an 18-m section namely C–C) (see Fig. 13 for this purpose). The numerical findings are presented in Figs. 14, 15 and 16 showing that any increase in the installation angle may results in the reduction of the maximum axial forces, bending moment, and shear forces.

Fig. 12 Vertical displacements of the tunnel crown in different installation angles



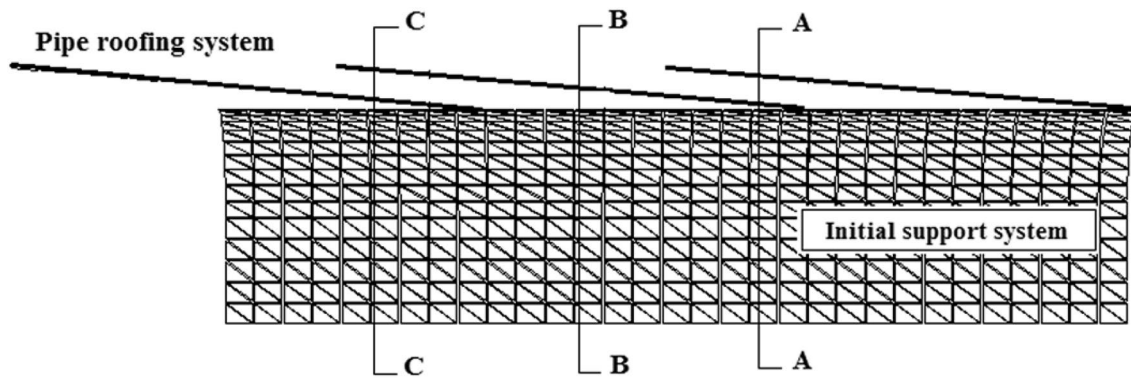


Fig. 13 Sections used for evaluation of the maximum internal forces in the initial support system

Fig. 14 Changes of the maximum axial force in the initial support system in different installation angles

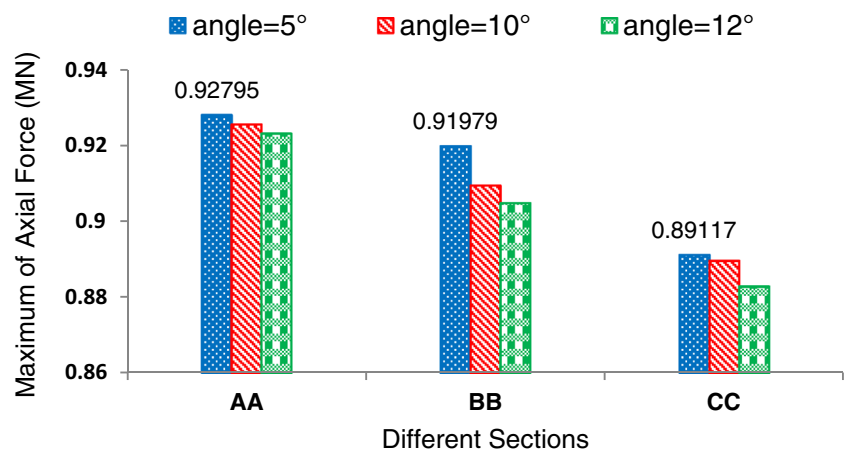
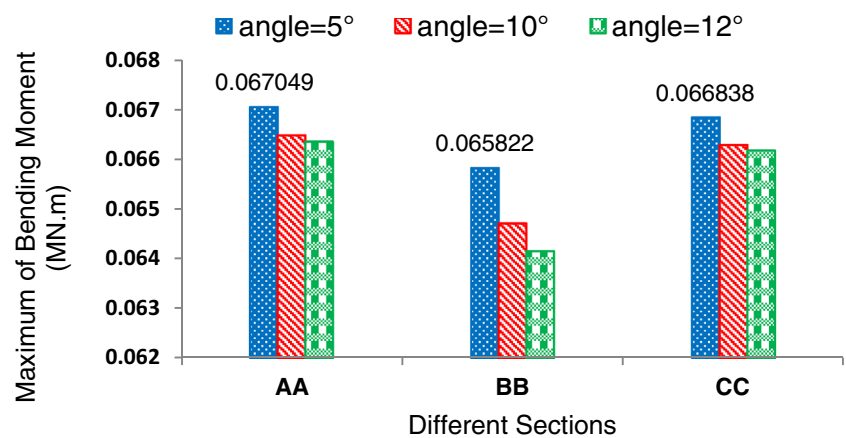


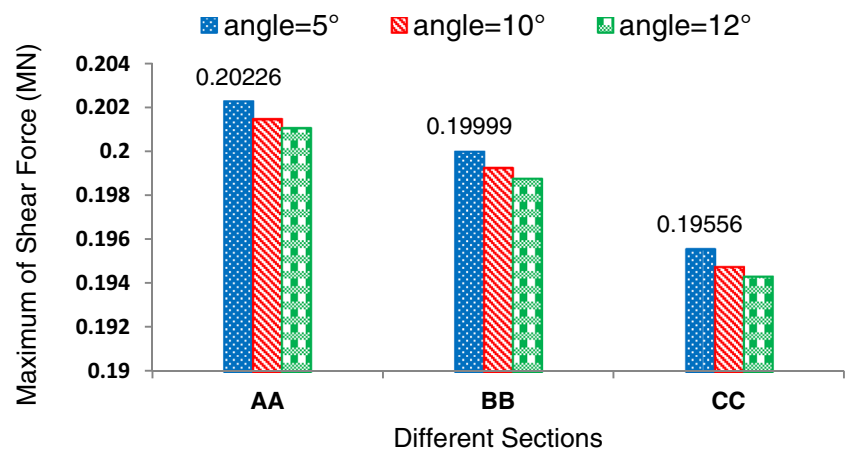
Fig. 15 Changes of the maximum bending moment in the initial support system in different installation angles



The installation angles may get bumped up to some degrees in an attempt to create more space for the next round of pipe installation. However, if they are extended more than what is required, the so-called effective length of the pipes may get decreased leading to more stages of pipe installation. In practice, several factors such as system stability, economical consideration and drilling machine

configuration should be evaluated to select a proper installation angle for pipes. In soft grounds, it is advised to use shorter pipes with larger installation angles. Longer bolts are also suggested to be installed at the tunnel face preventing any potential damage to the materials at the tunnel face.

Fig. 16 Changes of the maximum shear force in the initial support system in different installation angles



Assessing the role of the pipe's diameter

To evaluate the effect of variation in the pipe's diameter, the installation angle and transverse spacing are maintained at 5° and 40 cm, respectively. Any increase in the pipe's diameter results in a reduction of the vertical displacements in the tunnel crown for an excavation length of 24 m along the tunnel axis. The tunnel crown vertical displacements with different pipe's diameters are presented in Fig. 17. This figure indicates that the difference in the vertical displacements is quite higher where the overlapping area of the pipes is considered, coming from the fact that the number of pipes has considerably grown. Comparing the ground movements, from different cases, indicates that utilizing pipes with 114 mm diameter is much more effective than pipes with 60.3 mm diameter to control the excavation induced ground movements. Employing the former reduces the vertical displacements about 25% along the 10 m length of the tunnel. It is noteworthy that the maximum difference in vertical displacements occurred at 10 m and 18 m locations as shown

in Fig. 17. In terms of pre-supporting system configuration (see Fig. 7), in these locations a new set of pipes is installed which overlap with the old umbrella pipes. Additionally, a new set of face bolts is installed which interact with the old set of face bolts. It is, therefore, expected that the protective effects of pre-supporting measures increase in such overlapping areas.

The effect of pipe diameter on the maximum values of induced internal forces in the initial support system was also investigated. The maximum internal forces for different cross sections and diameters are presented in Figs. 18, 19 and 20. As can be seen the bigger the pipe diameter, the higher the maximum axial forces. Additionally, using pipes with bigger diameter results in lower maximum bending moment and shear force in all the three considered cross sections shown in Fig. 13. Axial force variation grows bigger where pipes are overlapped.

Pipe roofing system may be considered as a passive support system implying that bearing of the system come into action as soon as the surrounding ground starts displacing.

Fig. 17 Vertical displacements of the tunnel crown in case of applying pipes with different diameters

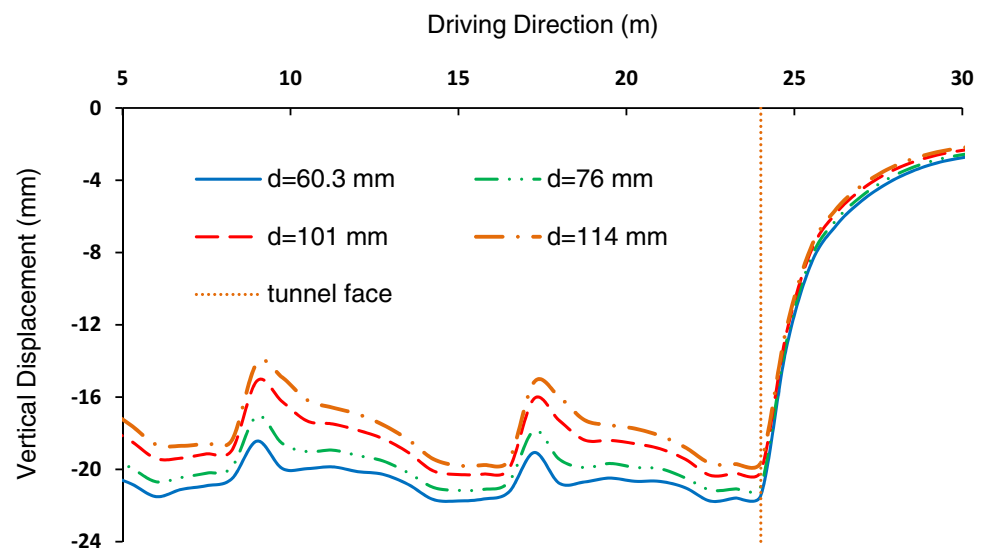


Fig. 18 Changes of the maximum axial force in the initial support system in different diameters

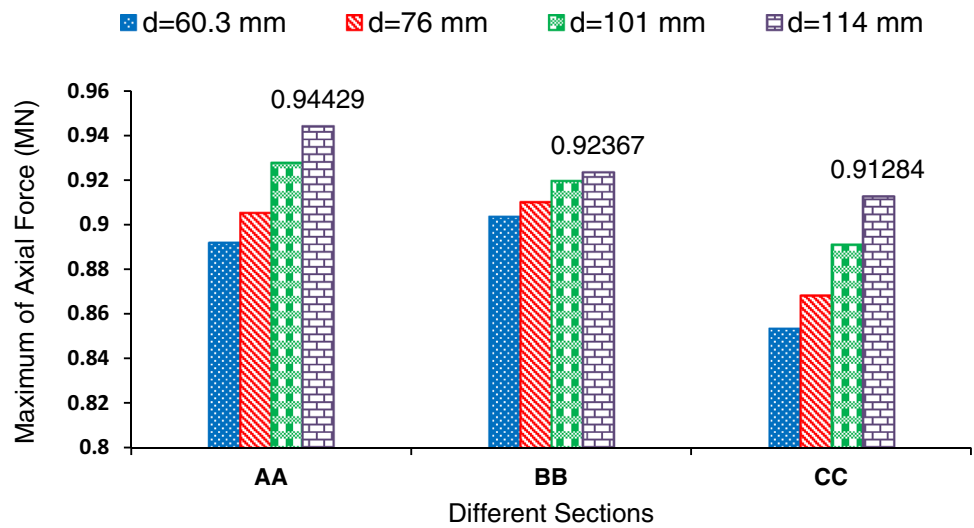


Fig. 19 Changes of the maximum bending moment in the initial support system in different diameters

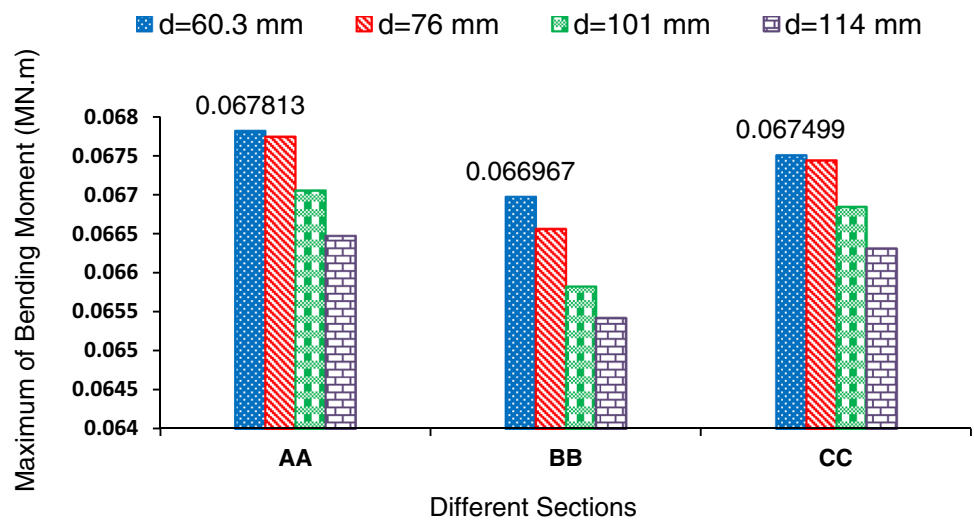
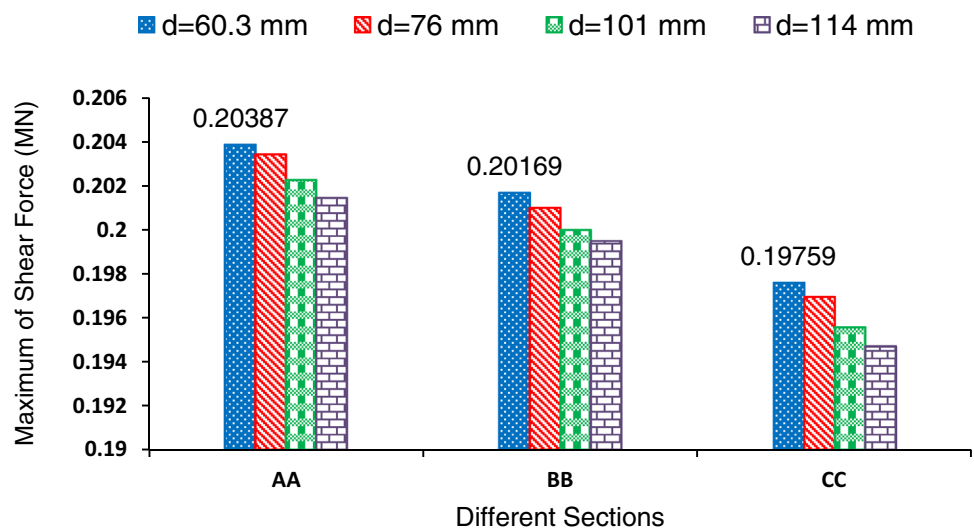


Fig. 20 Changes of the maximum shear force in the initial support system in different diameters



The bearing capacity of the pipe roofing system is proportional to the diameter of the pipes. This is because the bending strength of the system increases. Furthermore, to control ground settlement more effectively, utilizing pipes with bigger diameters is suggested.

Assessing the role of the transverse spacing between pipes

To evaluate the effect of transverse spacing among pipes on the performance of pipe roofing system, three transverse spacing 30 cm, 40 cm and 50 cm are considered. The pipe’s diameter is 101 mm and the installation angle is 5°, for all cases. The outcomes of the analyses show that as the transverse spacing among pipes increases, the vertical displacement of the tunnel crown, 24 m along the tunnel alignment, increases. Figure 21 shows the vertical displacement of the tunnel crown at different transverse spacing. According to this figure, the vertical displacement of the tunnel crown

increases by 10% as the transverse spacing changes from 30 to 50 cm at the 10-m section along the tunnel alignment. The number of pipes used at cases with 30 cm, 40 cm and 50 cm of transverse spacing is 29, 23 and 19, respectively.

The maximum values of the internal forces in different sections are extracted from numerical modelings. These data are then assessed to identify the effect of changes in the transverse spacing, between the pipes, on the maximum internal forces in the initial support system. The results are presented in Figs. 22, 23 and 24 indicating that the increase in the lateral spacing between the pipes leads to the reduction of the maximum axial forces and the increase of the maximum bending moment as well as the maximum shear force.

The transverse spacing between the pipes depends on the necessary support pressure as well as the quality of the surrounding ground. To benefit from the load bearing capacity of the ground, the distance must be chosen in a way that creates a minimum value of local arch between successive

Fig. 21 Vertical displacements of the tunnel crown in different transverse spacings

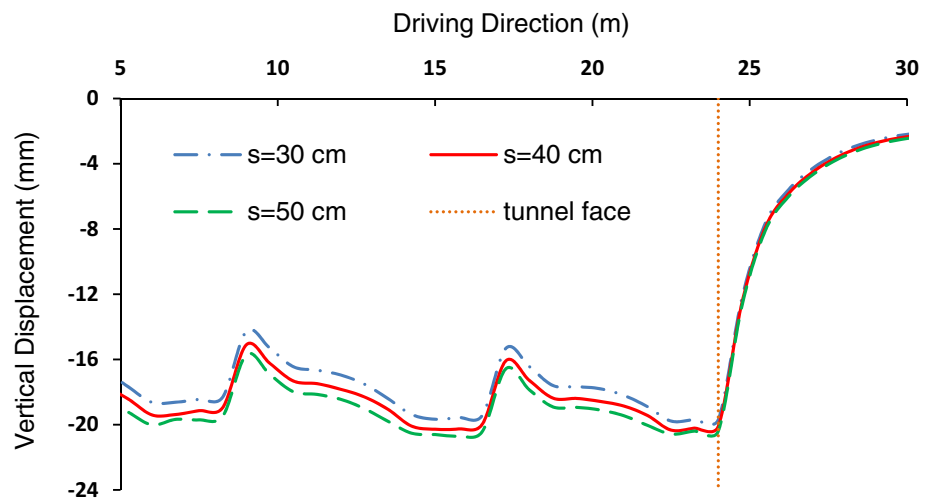


Fig. 22 Changes of the maximum axial force in the initial support system in different transverse spacings

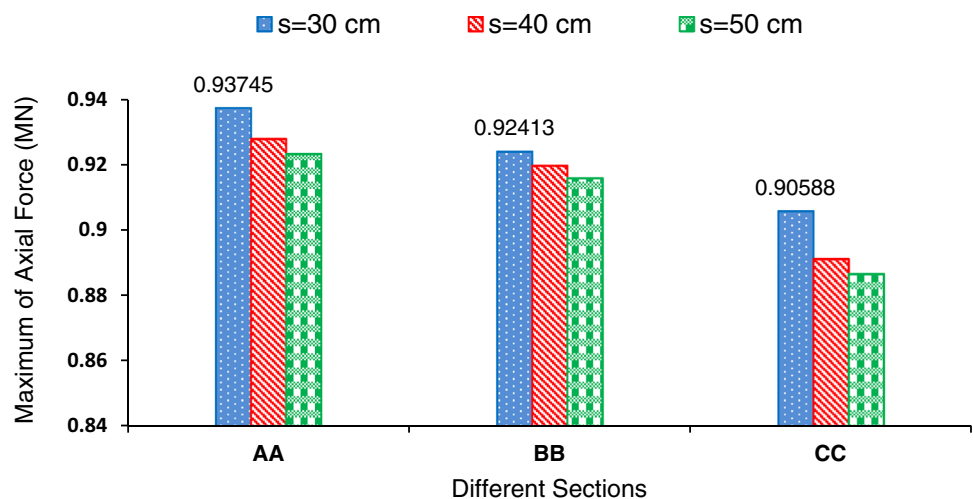


Fig. 23 Changes of the maximum bending moment in the initial support system in different transverse spacings

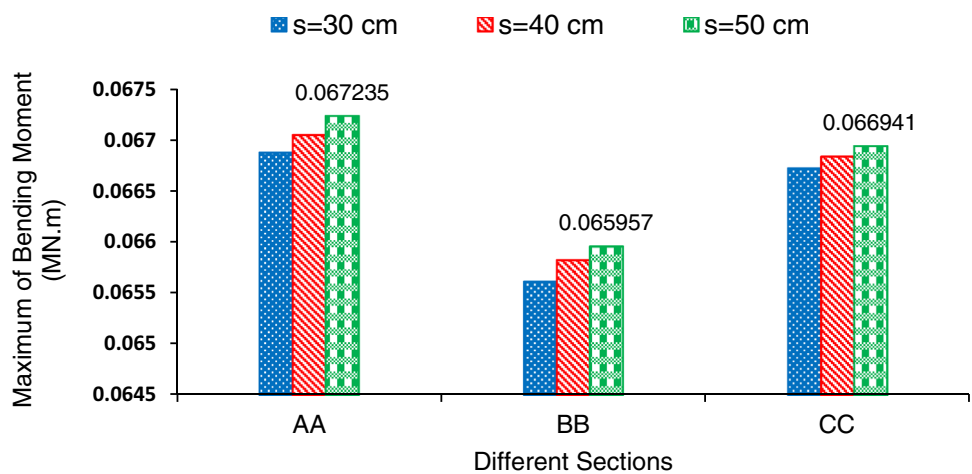
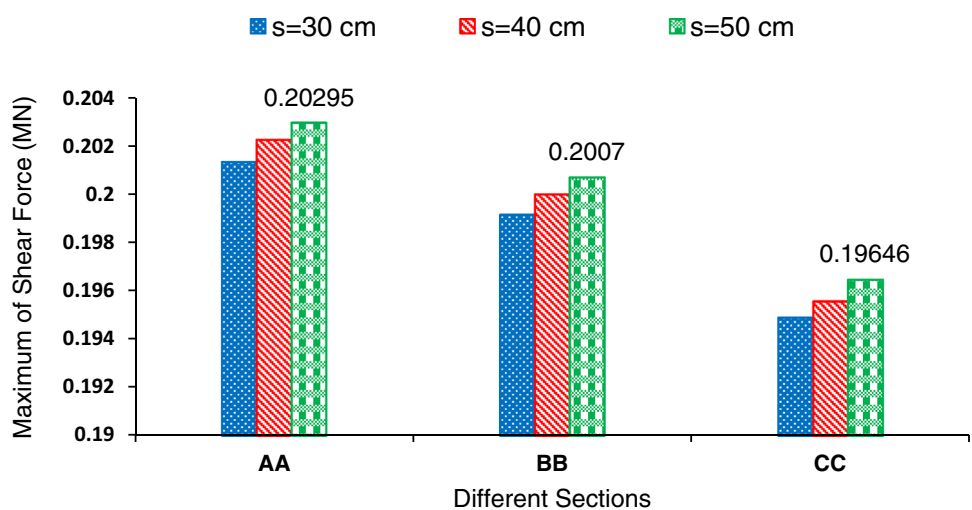


Fig. 24 Changes of the maximum shear force in the initial support system in different transverse spacings



pipes. Therefore, the designed shape of the tunnel can be obtained without causing significant local failure (Volkmann et al. 2006). The grouting pressure, and the number and diameter of the pipes are the other important factors that must be considered in determining the transverse spacing between the pipes. Decreasing the transverse spacing results in an increase in the number of pipes, which necessitates higher operational costs and higher installation time. Increasing the thickness and the diameter of the pipes could increase the bending stiffness and bending strength of the pipe roofing system. Therefore, to reduce the number of the required pipes the thickness and diameter of pipes may be increased.

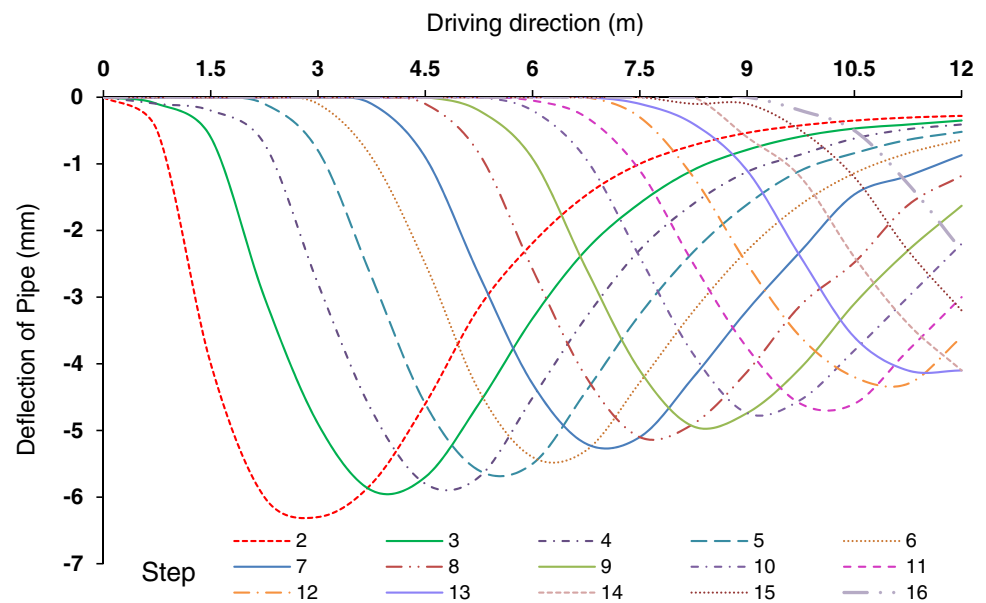
Assessing the role of the overlapping length

The protective umbrella created in the pipe roofing system, supports the unsupported span as well as the disturbed ground ahead of the tunnel face, meaning that this system transfer the loads in this area to the supported region (the

first foundation) and the ground further ahead of the face (the second abutment) (Volkmann et al. 2006; Schumacher and Kim 2013; Zhang et al. 2014). The overlapping length depends on the distance between the face and the second foundation (effective length) as well as the length of the second foundation, which are determined based on the tunnel shape and the ground condition. Accordingly, before the foundation effect decreases and the effective length of the pipes gets smaller than disturbed ground ahead of the face, a new set of pipes must be put in place just in time. When the overlapping length is increased, the greater proportion of the tunnel length will be supported by the overlapping pipes. This can enhance the supporting capability of the pipe roofing system. However, considering higher overlapping length may increase the costs of the pre-supporting method. This parameter, therefore, should be carefully optimized to satisfy both technical and economic aspects.

Figure 25 shows the deflection curves of the topmost pipe of the first pipe roofing stage in each step of excavation. Each of the presented curves depicts the bending of pipes for

Fig. 25 Deflection of the topmost pipe at the first round of pipe roofing in each step of excavation



the aforementioned excavation step. To draw these curves, the tunnel was excavated up to 12 m length (16 excavation steps) with no face bolts and the second stage of the pipe roofing system. As long as the effectiveness of the pipes is not reduced, as excavation proceeds pipes will bend in-between two specific points. The distance of these two points is the length that the pipes act as a supporting beam and transfer the loads towards the first and the second foundation. The maximum amount of the bending also occurs in 1.5 m distance ahead of the face. According to Fig. 25, after 12 excavation steps (9 m of the tunnel length) the effectiveness of the second foundation will fade and the new set of pipes must be put in place. Therefore, the overlapping length must be at least 3 m.

The required overlapping length should carefully be decided considering the imposed limitations. Additionally, the effective length of the pipes shall not be less than the length of the failure zone ahead of the tunnel face. Assuming that the tunnel face has undergone an active failure, the length of the failure zone, ahead of the face, may be determined using Eq. (1):

$$L = h \cdot \tan(45 - \varphi/2), \quad (1)$$

where the parameters L , h , and φ represent the length of the failed zone ahead of the face, the tunnel height and the internal friction angle of the surrounding ground, respectively. Using Eq. (1), the minimum overlapping length of the pipes is calculated to be 3.7 m.

Based on the bending curves shown in Fig. 25, it may be concluded that pipes behave like fixed beams at initial steps after installation. However, as the face advances the decrease in the pipes foundation length ahead of the face causes the pipes to behave like cantilever beams.

Analyzing the bearing capacity of supports

As mentioned in the previous section, pipes in the umbrella arch act like beams and transfer the ground induced loads to the initial support structure. Therefore, an important aspect in the design of pipe roofing system is to ensure that the utilized pipes and the initial support system are strong enough to sustain the applied loads. The stability of the initial support measures and the pipe elements are carefully investigated in this section.

Capacity diagrams of the initial support system

The Initial support system installed at the northern portal of Sabzkoooh tunnel consists of light-weight steel frame with 0.75 m lateral spacing, steel wire mesh with 100 square mm openings, and shotcrete with 20 cm in thickness. The specification of the initial support system components are presented in Table 4. The temporary composite support measure is modeled using shell elements with equivalent section characteristics and linear elastic material behavior with no failure limit. Therefore, to assess the stability of the tunnel

Table 4 The properties of the elements of the initial support system

Component of the initial support system	Compressive strength (kg/cm ²)	Elasticity modulus (kg/cm ²)
Shotcrete	210	218,820
Steel rib (ST37)	2400	2×10^6
Wire mesh	4000	2×10^6

support structure, the loads and moments in the composite support system are extracted from the numerical modeling. Then the bearing capacity diagrams are used, in this study, to evaluate the strength of the initial support system against the applied loads. In these diagrams, the horizontal axis shows the bending moment or shear force and the vertical axis represents the axial force. The upper bound on the horizontal axis shows the limit of the allowable interaction of bending moment–axial force or shear force–axial force under compressional failure, whereas the lower limit on the horizontal axis shows the limit of allowable interaction of these loads under tensile failure. Anywhere inscribed in these limits is then counted as safe area.

To draw the bending moment–axial force capacity diagram, a cross section of the initial support system is numerically modeled using Finite Element Method as illustrated in Fig. 26. Strength reduction factor for concrete is considered to account for the long-term load bearing capacity of the initial support system. As mentioned earlier in “Numerical modeling”, to draw the shear force–axial force capacity diagram, equations proposed by Hoek et al. (2008) and Carranza-Torres and Diederichs (2009) are used considering 1.5 as safety factor.

The results show that the maximum axial force is occurred in pipe overlapping area due to which Figs. 27 and 28 are

provided presenting the interaction diagrams, in different cases of the pipe roofing installation, in the 10 m section. As can be seen, all the pairs of bending moment–axial force and shear force–axial force are located within the permissible area which indicates that the initial support system is strong enough to cope with the applied loads. The bearing capacity diagrams have been provided for different sections in all of which the pairs of bending moment–axial forces and shear force–axial forces fall within the permissible area.

Assessing the bearing capacity of pipes

The stability of the pipes filled up with grout in the umbrella arch should also be investigated. Steel pipe is considered as the based material and the grout is transformed to an equivalent amount of steel using the ratio of their elasticity module (see Popov 1990). As an example for pipe with 76 mm diameter and 5 mm thickness, the area of the equivalent cross section is 1151 mm². Pipes are made of steel with yield stress around 392.26 MPa. Therefore, the maximum endurable force is calculated as:

$$F = \sigma_y A \rightarrow F = 392.26 \text{ (MPa)} \times 1151 \text{ (mm}^2\text{)} = 451.5 \text{ kN.}$$

Fig. 26 A schematic view of steel ribs, two layers of wire mesh and shotcrete (0.75 m)

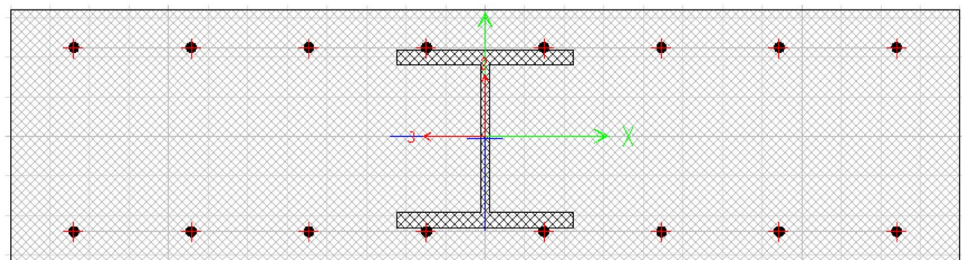


Fig. 27 The interaction diagram of bending moment–axial force of the initial support system in different states of a 10-m section

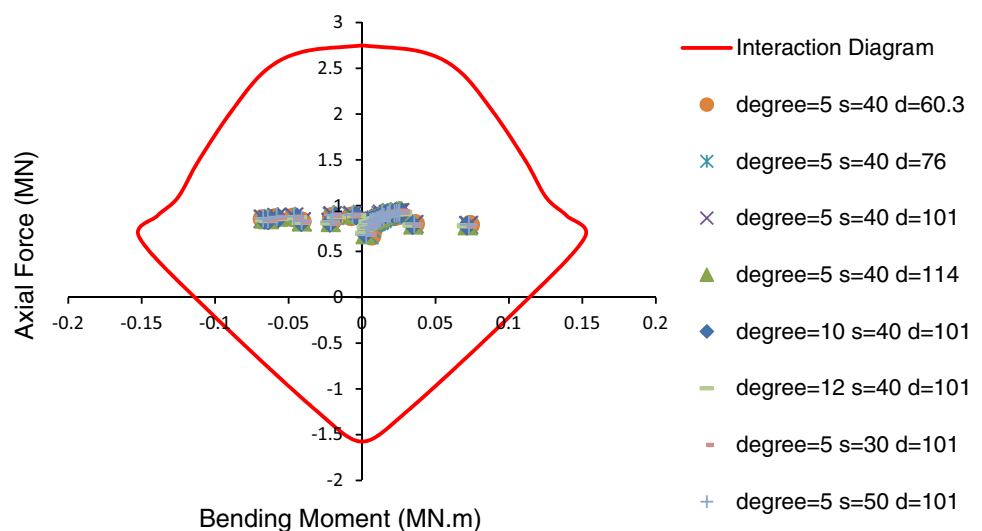
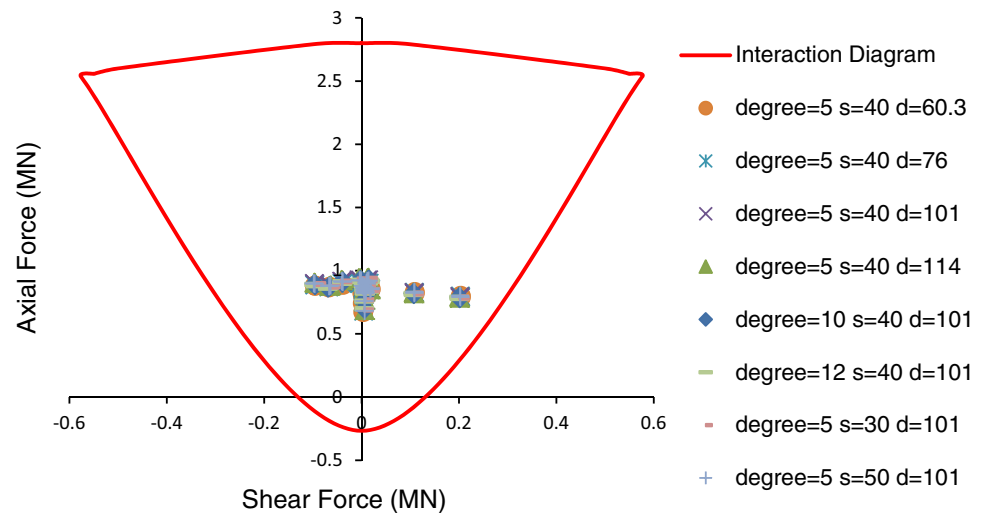


Fig. 28 The interaction diagram of bending moment–axial force of the initial support system in different states of a 10-m section



Outcomes of the performed numerical analyses indicated that the induced axial forces in the pipes are less than 300 kN. Hence, pipes are stable and strong enough to sustain the applied loads, during excavation.

Validating the axial forces induced in the initial support system

As mentioned, the umbrella arch system is installed prior to the tunnel excavation and ahead of the tunnel face. The applied loads and the boundary conditions of the pipes change during the stages of excavation. Therefore, none of the analytical solutions is capable of capturing the real interactions between the umbrella arches, the tunnel structure, and the surrounding rock/soil mass. However, a number of analytical solutions have been proposed to determine the induced internal forces in the tunnel support systems. Such analytical approaches can be used to verify the outcomes of the numerical modelings. Hence, to assess the accuracy of the numerical modelings, in this study, the induced axial forces in the initial support system are calculated using analytical solution and are compared against the counterparts extracted from the numerical modeling.

To calculate the induced axial force in the initial support system, the equation developed by Einstein and Schwartz (1979) is applied, as:

$$T = \frac{PR}{2} \left\{ (1 + K)(1 - a_0) + (1 - K)[1 + 2a_2^*] \cos 2\theta \right\}, \quad (2)$$

where R is the tunnel radius, T is the axial force, P is the vertical stress, K is the ratio of the horizontal stress to the vertical stress, θ is the angular location (ccw w.r.t horizontal), a_0 , and a_2 are dimensionless coefficients, determination of which are explained by Schwartz and Einstein (1980).

A few assumptions were considered for deriving the above-mentioned equation. Firstly, it was assumed that the

surrounding ground is an elastic, isotropic and homogeneous medium. Plane strain condition was also considered. It was also assumed that the support system and excavation are simultaneously applied (Einstein and Schwartz 1979).

To evaluate the development of the internal forces in the support system, based on the actual excavation sequence, the stress relaxation before the installation of the support system and the expansion of the plastic zone around the tunnel should be considered. Therefore, to consider the reduction of the internal forces due to the stress relaxation and the increase of the internal forces due to the development of the plastic zone, delay factor, λ_d , and yield factor, λ_y , are suggested, respectively. The procedures for determining these factors have been well explained in relevant references (Schwartz and Einstein 1980; Kim and Eisenstein 2006). The corrected axial force, T_f , can, therefore, be obtained by (Schwartz and Einstein 1980):

$$T_f = \lambda_d \cdot \lambda_y \cdot T. \quad (3)$$

As the analytical equations are presented to be used in a circular tunnel section, in this study, the results obtained from analytical equations with equivalent circular section were compared to that of numerical modeling for equivalent circular section and horseshoe section.

The comparison is carried out in two different conditions: at the first one, Eq. (2) is used for computing the axial force (no correction factor was used) and consequently the numerical modeling is performed assuming plane strain state and the support system is immediately installed after excavation. In numerical modeling for the equivalent circular section, the surrounding ground is assumed to behave in an elastic way. This is to apply the assumption considered for deriving Einstein and Schwartz (1979) equations. Moreover, the changes in the stress level are assumed to be zero. In other words, the vertical stress is assumed to be constant (height of overburden: 22.5 m) in the model. For modeling the

horseshoe section, different layers of overburden are modeled as shown in Table 1 and the vertical stress is considered as overburden-induced stress for the corresponding depth.

Figure 29 shows the obtained values of the axial force through different methods assuming that the support system is immediately installed after excavation. It can be seen that the axial force obtained through analytical methods (shown by ‘Ana’) is well matched to that of numerical modeling for an equivalent circular section (shown by ‘num-1’). The axial force value obtained through numerical modeling for a horseshoe section (shown by ‘num-2’) is approximately 10% more than the other cases, which is due to the increased level of stress by depth as well as the difference in the excavation induced stresses around the horseshoe and circular sections.

Correction factors (Eq. 3) were used to predict the axial forces in the second case. This is to take into account the stress release before the installation of support systems and

the development of the yielding zone. The actual excavation sequence is considered in the numerical modeling. The obtained values of axial forces using analytical method with correction factors (‘Ana’), the numerical modeling of equivalent circular section without pipe roofing system (‘num-1’), and the numerical modeling of the horseshoe section without pipe roofing system (‘num-2’) and the numerical modeling of horseshoe section with the installation of the pipe roofing system and face bolts (‘num-3’) are presented in Fig. 30. It should be mentioned that in this case, in the numerical modeling of the equivalent circular section like modeling of the horseshoe section, the consecution of geological layers is taken into account. Hence, the vertical stress is considered to be the same as the overburden-induced stress in the corresponding depth. The Mohr–Coulomb elasto-plastic yield model is also used to replicate the behavior of the surrounding ground.

Fig. 29 Induced axial force in the initial support system assuming the immediate installation of support after excavation

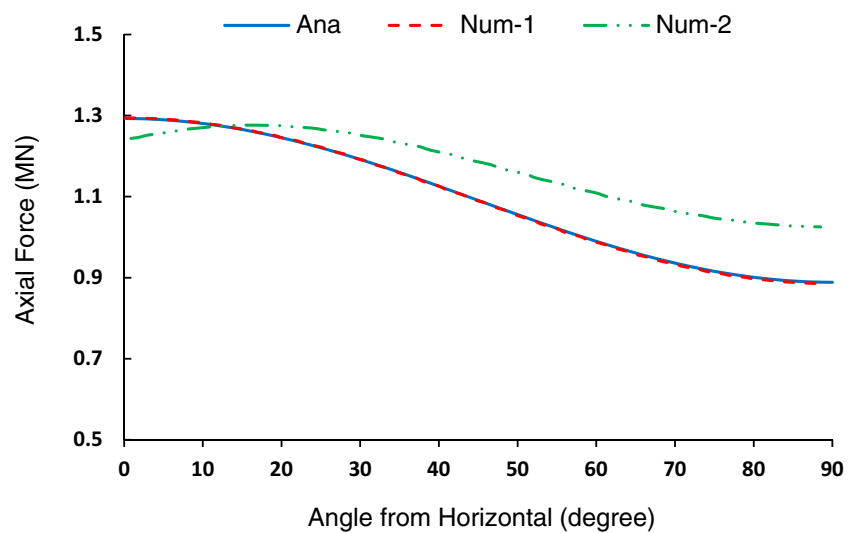
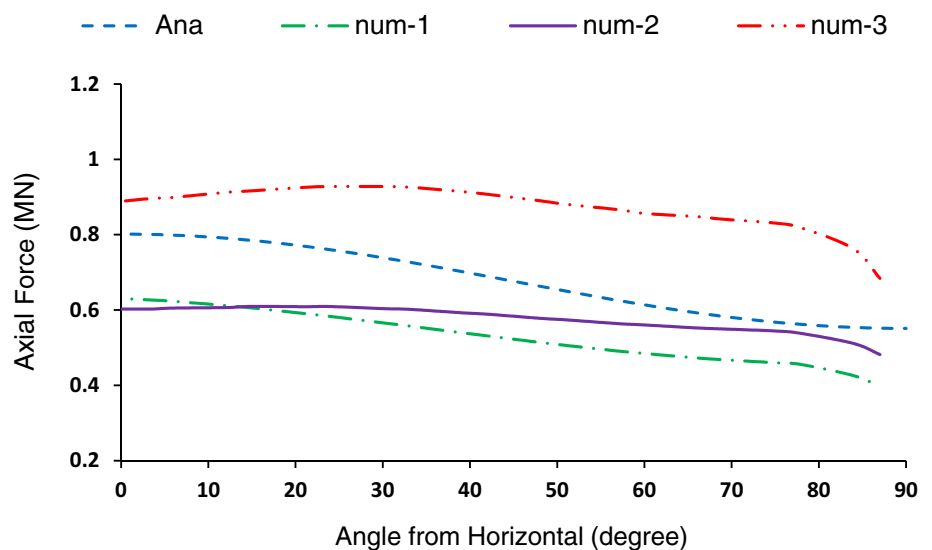


Fig. 30 Axial force induced in the initial support system considering the stress release before installation of support system as well as the development of the yielding zone



As can be understood from Fig. 30, the predicted axial forces using analytical equations ('Ana') well consist with that of numerical modeling for the equivalent circular section ('num-1'). However, the values of axial forces obtained through the analytical approach are approximately 25% more than that of the numerical modeling for the equivalent section which is in good accordance with the results of studies by Kim and Eisenstein (2006). The minor discrepancy between the values and the trend of the axial force in the numerical modeling of the horseshoe section ('num-2') and the equivalent section ('num-1') can be justified considering the difference in the section type. From Fig. 30, it can be seen that the induced axial force in the initial support system in the case with pipe roofing system and face bolts ('num-3') are more than those of other cases which is explained by the reduced displacements around the tunnel and the transferred loads by pipes.

The consistency between the axial forces obtained through the analytical solution and numerical modeling, indeed, proves the reliability of the performed numerical modelings and their outcomes.

Conclusions

Using pipe roofing system and face bolts result in a considerable decrease in the tunnel convergence. Based on the outcomes of this study, using pipe roofing system and face bolting approach compared to the lack of pre-supporting system, eventuated in a 57% and a 74% of reduction in the vertical displacements in the tunnel crown and the ground surface settlement in 14 m of the tunnel route, respectively.

Outcomes of the numerical modeling indicated that an increase in the installation angle of the pipes leads to an increase in the vertical displacements of the tunnel crown. According to the obtained results, increasing the pipe angle from 5° to 12° resulted in a 12% increase in the vertical displacement of the crown in 11 m of the tunnel route. However, increasing this angle led to a decrease of the maximum axial force, bending moment and shear force induced in the initial support system.

Increasing the diameter of the pipes decreases the vertical displacement in the tunnel crown. The results revealed that using pipes with 114 mm diameter with regard to the pipes of 60.3 mm caused around 25% reduction in the tunnel crown vertical displacement along 10 m of the tunnel route. Moreover, increasing the pipes diameter resulted in increasing the maximum axial force as well as decreasing the maximum bending moment and the maximum shear force induced in the initial support system. The diameter of the pipes has the most influential impact on the amount of the vertical displacements in the tunnel crown.

Increasing the transverse spacing of the pipes also resulted in increasing the vertical displacements in the tunnel crown. The results showed that a 10% increase in the amount of the vertical displacements in the tunnel crown along 10 m of the tunnel route is observed, when the transverse spacing of the pipes is increased from 30 to 50 cm. Additionally, increasing the transverse spacing of the pipes reduces the maximum axial force and increase the maximum bending moment and the shear force induced in the initial support system.

The application of the pipe roofing system and face bolts led to increase in the axial force induced in the initial support system, especially in the overlapping area. This study indicated that using pipe roofing and face bolting system caused a 50% increase in the amount of the axial forces induced in the initial support system.

Analyses based on capacity diagrams indicated that the initial composite support structure consisting of 200 mm shotcrete, which is reinforced with two layers of wire mesh ($\Phi 100$ mm @ 5 mm), and steel frames with 0.75 m lateral spacing, is strong enough to sustain the applied loads. Additionally, a pre-supporting system with pipe with 75–100 mm diameter, 400–500 mm lateral transverse spacing, 5°–10° installation angle, and 3.0–5.0 m overlapping can provide a stable arch to control the tunnelling induced displacement at the northern portal of Sabzkoo tunnel.

References

- Ahuja V, Sterling R (2008) Numerical modelling approach for micro-tunnelling assisted pipe-roof support system. In: The World Tunnel Congress 2008, underground facilities for better environment and safety, India
- Aksoy CO, Onargan T (2010) The role of umbrella arch and face bolt as deformation preventing support system in preventing building damages. *Tunn Undergr Sp Technol* 25(5):553–559. <https://doi.org/10.1016/j.tust.2010.03.004>
- Aliabadian Z, Sharafisafa M, Nazemi M, Rezazadeh A (2015) Numerical analyses of tunnel collapse and slope stability assessment under different filling material loadings: a case study. *Arabian J Geosci* 8:1229–1242. <https://doi.org/10.1007/s12517-014-1286-1>
- Aydin A, Ozbek A, Cobanoglu I (2004) Tunnelling in difficult ground: a case study from Dranz tunnel, Sinop, Turkey. *Eng Geol* 74(3):293–301. <https://doi.org/10.1016/j.enggeo.2004.04.003>
- Barla M, Bzowka J (2013) Comparing numerical alternatives to model jet grouting in tunnels. *Electron J Geotech Eng* 18:2997–3008
- Bruce DA, Boley DL, Gallavresi F (1987) Chapter 51—New developments in ground reinforcement and treatment for tunnelling. In: Paper presented at the proceedings of the RETC conference
- Carranza-Torres C, Diederichs M (2009) Mechanical analysis of circular liners with particular reference to composite supports. For example, liners consisting of shotcrete and steel sets. *Tunn Undergr Sp Technol* 24(5):506–532. <https://doi.org/10.1016/j.tust.2009.02.001>
- Chakeri H, Unver B (2014) A new equation for estimating the maximum surface settlement above tunnels excavated in soft ground.

- Environ Earth Sci 71(7):3195–3210. <https://doi.org/10.1007/s12665-013-2707-2>
- Coulter SNP (2004) Influence of tunnel jet-grouting on ground deformations at the Aeschertunnel. The University of Alberta, Alberta
- Coulter S, Martin CD (2006) Effect of jet-grouting on surface settlements above the Aeschertunnel, Switzerland. *Tunn Undergr Sp Technol* 21(5):542–553. <https://doi.org/10.1016/j.tust.2005.07.005>
- Eftekhari A, Taromi M, Saeidi M (2014) Uncertainties and complexities of the geological model in slope stability: a case study of Sabzkuh tunnel. *Int J Min Geo-Eng* 48:69–79. <https://doi.org/10.22059/ijmge.2014.51807>
- Einstein HH, Schwartz CW (1979) Simplified analysis for tunnel supports. *J Geotech Geoenviron* 105:499–518
- Elyasi A, Javadi M, Moradi T, Moharrami J, Parnian S, Amrac M (2016) Numerical modeling of an umbrella arch as a pre-support system in difficult geological conditions: a case study. *Bull Eng Geol Environ* 75:211–221. <https://doi.org/10.1007/s10064-015-0738-5>
- Ercelebi SG, Copur H, Ocak I (2011) Surface settlement predictions for Istanbul metro tunnels excavated by EPB-TBM. *Environ Earth Sci* 62(2):357–365. <https://doi.org/10.1007/s12665-010-0530-6>
- Hefny AM, Tan WL, Ranjith P, Sharma J, Zhao J (2004) Numerical analysis for umbrella arch method in shallow large scale excavation in weak rock. *Tunn Undergr Sp Technol*. <https://doi.org/10.1016/j.tust.2004.02.097>
- Hoek E (2004) Numerical modeling for shallow tunneling in weak rock. Discussion paper 3
- Hoek E, Carranza-Torres C, Diederichs M, Corkum B (2008) The 2008 Kersten Lecture Integration of geotechnical and structural design in tunneling. In: 56th Annual geotechnical engineering conference, pp 1–53
- Itasca Consulting Group (1997) FLAC^{3D}, Fast Lagrangian analysis of continua in 3 dimensions. Itasca Consulting Group, Minneapolis, US
- Jaky J (1948) Pressure in silos. In Proceedings of the 2nd international conference on soil mechanics and foundation engineering, vol 1, pp 103–107
- Juneja A, Hegde A, Lee FH, Yeo CH (2010) Centrifuge modelling of tunnel face reinforcement using forepoling. *Tunn Undergr Sp Technol* 25:377–381. <https://doi.org/10.1016/j.tust.2010.01.013>
- Kim HJ, Eisenstein Z (2006) Prediction of tunnel lining loads using correction factors. *Eng Geol* 85:302–312. <https://doi.org/10.1016/j.enggeo.2006.03.001>
- Muraki Y (1997) The umbrella method in tunnelling. Doctoral dissertation, Massachusetts Institute of Technology
- Ocak I (2008) Control of surface settlements with umbrella arch method in second stage excavations of Istanbul Metro. *Tunn Undergr Sp Technol* 23:674–681. <https://doi.org/10.1016/j.tust.2007.12.005>
- Ocak I (2013) Interaction of longitudinal surface settlements for twin tunnels in shallow and soft soils: the case of Istanbul Metro. *Environ Earth Sci* 69(5):1673–1683. <https://doi.org/10.1007/s12665-012-2002-7>
- Ocak I (2014) A new approach for estimating the transverse surface settlement curve for twin tunnels in shallow and soft soils. *Environ Earth Sci* 72(7):2357–2367. <https://doi.org/10.1007/s12665-014-3145-5>
- Oke J, Vlachopoulos N, Diederichs MS (2014) Numerical analyses in the design of umbrella arch systems. *J Rock Mech Geotech Eng* 6:546–564. <https://doi.org/10.1016/j.jrmge.2014.09.005>
- Peila D, Pelizza S (2005) Ground reinforcing for tunneling the example of steel pipe umbrella. ITA-AITES Training Course, Istanbul
- Pizzarotti EM (2001) Advantages and ground improvement effects of RPUM. In: The symposium on reinforced protective umbrella Methods (RPUM) in tunnelling, Seoul, Korea
- Popov EP (1990) Engineering mechanics of solids. Prentice Hall, Englewood Cliffs
- RWC C&BP (2009) Geotechnical report of Sabzkuoh tunnel. The Regional Water Company of Chaharmahal and Bakhtiari Province, Shahrekord, Iran
- Salmi EF, Nazem M, Giacomini A (2015) A practical method to control the formation of sinkhole subsidence—The Dolaei road tunnel case study. In: Proceedings of the 13th international congress of rock mechanics, ISRM Congress, Montreal, Canada
- Salmi EF, Nazem M, Giacomini A (2017) A numerical investigation of sinkhole subsidence development over shallow excavations in tectonised weak rocks: the Dolaei tunnel's excavation case. *Geotech Geol Eng* 35:1685–1716. <https://doi.org/10.1007/s10706-017-0202-3>
- Schumacher FP, Kim E (2013) Modeling the pipe umbrella roof support system in a Western US underground coal mine. *Int J Rock Mech Min Sci* 60:114–124. <https://doi.org/10.1016/j.ijrmms.2012.12.037>
- Schwartz CW, Einstein HH (1980) Simplified analysis for ground-structure interaction in tunneling. In: The 21st US symposium on rock mechanics (USRMS), American Rock Mechanics Association, Rolla, Missouri, pp 787–796
- Shin JH, Choi YK, Kwon OY, Lee SD (2008) Model testing for pipe-reinforced tunnel heading in a granular soil. *Tunn Undergr Sp Technol* 23:241–250. <https://doi.org/10.1016/j.tust.2007.04.012>
- Song KI, Cho GC, Chang SB, Lee IM (2013) Beam-spring structural analysis for the design of a tunnel pre-reinforcement support system. *Int J Rock Mech Min Sci* 59:139–150. <https://doi.org/10.1016/j.ijrmms.2012.12.017>
- Starfield AM, Cundall PA (1988) Towards a methodology for rock mechanics modeling. *Int J Rock Mech Min Sci Geomech Abstr* 25:99–106
- Taromi M, Eftekhari A, Hamidi JK (2015) Evaluation of geological model in construction process of Sabzkuh tunnel (case study in Iran). *Eng Geol Soc Territory* 6:599–610
- Taromi M, Eftekhari A, Hamidi JK, Aalianvari A (2017) A discrepancy between observed and predicted NATM tunnel behaviors and updating: a case study of the Sabzkuh tunnel. *Bull Eng Geol Environ* 76(2):713–729. <https://doi.org/10.1007/s10064-016-0300-1>
- Türkmen S, Özgüzel N (2003) Grouting a tunnel cave-in from the surface: a case study on Kurtkulağı irrigation tunnel, Turkey. *Tunn Undergr Sp Technol* 18(4):365–375
- Volkman GM, Schubert W (2008) Tender document specifications for pipe umbrella installation methods. In: The 34th ITA-AITES world tunneling congress, underground facilities for better environment and safety, vol 1, pp 285–293
- Volkman GM, Button EA, Schubert W (2006) A contribution to the design of tunnels supported by a pipe roof. In: Golden rocks, the 41st US symposium on rock mechanics (USRMS), American Rock Mechanics Association
- Wang H, Jia J (2008) Analytical method for mechanical behaviors of pipe roof reinforcement. In: International conference on information management, innovation management and industrial engineering vol 3, pp 352–357, IEEE. <https://doi.org/10.1109/iciii.2008.96>
- Wang H, Jia J (2009) Face stability analysis of tunnel with pipe roof reinforcement based on limit analysis. *EJGE* 14:1–15
- Wong H, Trompille V, Subrin D, Guilloux A (1999) Tunnel face reinforced by longitudinal bolts: analytical model and in situ

data. In: International symposium-geotechnical aspects of underground construction in Soft Ground-IS Tokyo

Zhang G, Yang J, Gou D (2010) A shell model for pipe roof reinforcement analysis in shallow tunnel. *EJGE* 15:1625–1640

Zhang Z, Li H, Liu H, Li G, Shi X (2014) Load transferring mechanism of pipe umbrella support in shallow-buried tunnels. *Tunn Undergr Sp Technol* 43:213–221. <https://doi.org/10.1016/j.tust.2014.05.018>

Publisher's Note Springer Nature remains neutral with regard to jurisdictional claims in published maps and institutional affiliations.